Renewable Energy 141 (2019) 678–692

Contents lists available at ScienceDirect

Renewable Energy

journal homepage: www.elsevier.com/locate/renene

Components and design guidelines for solar cooling systems: The experience of ZEOSOL

Valeria Palomba [a], Ursula Wittstadt [b], Antonino Bonanno [a], Mirko Tanne [b], Niels Harborth [c], Salvatore Vasta [a, *]

[a] Consiglio Nazionale delle Ricerche (CNR), Istituto di Tecnologie Avanzate per l'Energia "Nicola Giordano" (ITAE), Via Salita S. Lucia sopra Contesse n. 5, 98126, Messina, Italy
[b] Fahrenheit AG, Siegfriedstr. 19, 80803, Munich, Germany
[c] AkoTec Produktionsgesellschaft mbH, Grundmühlenweg 3, 16278, Angermünde, Germany

ARTICLE INFO

Article history:
Received 29 November 2018
Received in revised form
4 March 2019
Accepted 4 April 2019
Available online 9 April 2019

Keywords:
Solar cooling
Hybrid chillers
Energy efficiency
Experimental
System design
HVAC

ABSTRACT

In this paper, the activity carried out within the H2020 project ZEOSOL is introduced. Making use of the lessons learned from previous solar cooling projects, an advanced hybrid solar cooling system was developed. It consists of a thermal and an electric unit in parallel integrated in a single unit with the dry-cooler. ZEOSOL is based on commercial components but was optimised in order to guarantee optimal seasonal performance, high reliability (and therefore reduced maintenance) and easy installation. The components of the system were experimentally tested in the laboratories of AkoTec, CNR ITAE and Fahrenheit, with a specific attention to the definition of performance maps as a function of operating and design parameters. During the tests of each component, possible control strategies and rules were identified. Subsequently, a simplified sizing tool was developed, which can be adapted to different configurations and climates and takes into account user-experience for different stakeholders, such as engineers and installers. The methodology implemented is described, in order to be used as a guideline for the definition of standard sizing procedures for solar cooling systems. As exemplary cases, the results for three different climates (Athens, Berlin and Ryiad) are also presented.

© 2019 The Authors. Published by Elsevier Ltd. This is an open access article under the CC BY license (http://creativecommons.org/licenses/by/4.0/).

1. Introduction

The exploitation of solar energy in buildings is a widely explored field, with the first applications dating back over one century ago [1,2]. The application of solar energy to cover the cooling demand of buildings is also a well-known concept, for either residential, commercial or industrial fields. In particular, two main competing methods for cooling production starting from solar energy are possible: PV cooling and solar thermal cooling [1,3], whose technical and economic gap is continuously narrowing [4,5]. Among solar thermal technologies, different solutions are possible, mainly differing for the thermal cycle applied, e.g. absorption or adsorption. Several layouts and chillers have been investigated within the years towards the development, improvement and optimization of sorption cycles for cooling production from solar heat, as testified by the intense research for both adsorption [6–9] and absorption systems [10–14] at components and system levels, and by the number of reviews on the topic, which allow having a complete overview of the recent advancements and future trends for the topic [15–17]. Nonetheless, efforts in the research of novel materials [18], advanced components [19,20] and optimised cycles [21,22] and controls [23] are still on-going with the aim of increasing the overall performance of these type of systems.

For instance, recently, several novel materials for heat transformation and storage were proposed at lab-scale, such as novel zeotypes (AlPOs, SAPOs) [18,20,24], MOFs [25–27] and composites [28–30], with superior water uptake performance. For some of these, cycle stability has already been proven [31], as well as the possibility to employ them under realistic conditions [24]. In Ref. [32] authors improved the performance of composite materials based on a silica gel loaded with $CaCl_2$ and evaluated their multi-cycle stability in conditions of a solar heat storage system, similar to the conditions investigated here. However, long-term assessment and compatibility with constructive materials of these new materials have not been still adequately addressed to foresee the

* Corresponding author.
E-mail address: salvatore.vasta@itae.cnr.it (S. Vasta).

https://doi.org/10.1016/j.renene.2019.04.018
0960-1481/© 2019 The Authors. Published by Elsevier Ltd. This is an open access article under the CC BY license (http://creativecommons.org/licenses/by/4.0/).

Nomenclature

A	Aperture area, m^2
a_1	Heat loss coefficient $W/(m^2K)$
a_2	Heat loss coefficient $W/(m^2K^2)$
c_p	Specific heat, kJ/kg K
E	Electric power, kW
G	Solar radiation, W/m^2
$\dot{m}$	Mass flow rate, kg/s
t	Time, s
v	Speed, m/s
η_0	Collectors efficiency, adm

Subscripts

amb	ambient
coll	collectors
comp	compression
el	electrical
in	inlet
out	outlet
th	thermal

Abbreviations

COP	Coefficient of Performance
DC	Dry Cooler
EER	Energy Efficiency Ratio
HP	Heat Pipe
HT	High Temperature
LT	Low Temperature
MT	Medium Temperature
STC	Single Tube Collector

application in commercial systems [33,34].

Indeed, reliability, costs and a long lifetime of commercial systems are One of the most critical issues to be solved to ensure that the overall life-cycle impact of an adsorption cooling system is effectively lower than traditional or other renewable-based cooling systems [35].

However, despite the research on materials and components, design aspects as well as operation optimization can affect the overall performance, cost effectiveness and system reliability more than innovative and performant materials [4,36].

In this regard, efficient heat rejection has been long established as a key point for the exploitation of solar heat in sorption cooling, especially in severe weather conditions [37–39]. Moreover, the larger energy consumption in solar cooling systems is due to the electricity needed for the operations of fans in the air/water heat rejection devices [40]. Possible methods for condensation and adsorption heat rejection are wet cooling towers, dry coolers and geothermal probes [37,41]. However, both wet cooling towers and geothermal probes suffer from severe regulations and legislative issues, which make the dry coolers a more convenient solution [17]. For the application of these system as an effective means of heat rejection for solar cooling, two are the main competing challenges [17]: low electricity consumption with control capacity for part load and integration of all components into a complete system.

Despite these open issues, the technological and economic feasibility of solar sorption technology has been established and several different installations exist up to now, proving that the technology is mature enough. For instance, in Ref. [42] the possibility of running a solar adsorption cooling system in residential buildings with a solar fraction ranging from 80% to 100% in different warm climates was proven. Similarly, in Ref. [12], techno-economic evaluations on a solar cooling system employing a single-effect absorption chiller revealed the sustainability of the solution in the climates of Abu Dhabi and Phoenix.

However, as already stated in Ref. [2], the massive diffusion of these systems does not depend merely on the technical and economic aspects: the possibility of providing a systematic approach for the design and installation of the system in different climates, easily manageable even by professionals who are not expert on the specific technology is a relevant issue to be addressed as well.

Up to now, the design of a solar cooling system has been carried out by dynamic simulation tools, mainly developed in TRNSYS or EnergyPlus. A good overview of literature contributions is reported in Ref. [43]. In particular, these tools were used for energy and techno-economic analysis since experimental evaluations are usually quite complex and expensive.

In Ref. [10] authors present a thermo-economic analysis and multi-objective optimization as well as energy-exergy analyses of a single-effect solar absorption cooling system. Xu and Wang [11] realized a complex model of the variable effect LiBr-water absorption chiller implemented by means of artificial neural network (ANN) based on 450 groups of experimental data. In Ref. [12] Bellos and Tzivanidis investigated the performance and the costs of a single stage absorption chiller based solar cooling system in ten cities by conducting an accurate analysis with the commercial software TRNSYS. Similarly, a TRNSYS model has been implemented in Ref. [36] to quantify the effect of different operational and design parameters on the overall performances and costs of solar cooling systems in three different Italian cities (Milan, Rome, and Messina).

In Ref. [43] authors introduce a detailed simulation model written in MatLab for energy, economic, and environmental performance assessment of a polygeneration systems, based on both adsorption and as well as absorption chiller technologies. A lumped parameter model is utilized in order to simulate the performance of the adsorption chiller [44] in a solar thermal cooling system coupled with flat plate solar collectors. The same model allowed authors to simulate and compare a solar electrical cooling system coupled with photovoltaic modules. It is clear that the present approach is suitable for research and detailed optimization purposes, but is within the scope of design engineering, which is the one of the missing aspects for the massive dissemination of adsorption solar cooling.

In addition to these models, self-developed codes have been employed for the optimization of layout and operation [23]. Within IEA-SHC Task 53, a tool was developed to enable a comparable performance assessment of solar cooling and heating systems on technical and economic level [45], but it is still based on monthly results from simulations. What all these tools have in common is their high level of detail and reliability, but they lack simplicity and the possibility to guarantee the flexibility in the quick design of the main components of the system in different climates starting from a reduced set of data. Therefore, an attempt was made within IEA-SHC Task 48, with the development of the PISTACHE tool [46], which is however nowadays out-dated, in terms of solar collectors and sorption chillers available for the sizing.

In this context, the European H2020 project ZEOSOL aims at developing a market-ready solution for affordable solar cooling and heating purposes. The proposed solution exploits adsorption technology that guarantees optimal seasonal performance, high

reliability, reduced maintenance needs and allows an easy and standardized installation. Consequently, design and installation are mistake-proof thanks to the integration of all the components (solar collectors, adsorption chiller and larger dry cooler) and the development of a simplified, easy-to-use tool for the sizing.

Accordingly, in this paper we describe the experiences gained during the project in the development of the single components as well as the design and optimization of the whole system.

2. System description

The typical layout of a solar cooling system consists of (i) a solar section, including solar collectors and a hot storage tank, (ii) the thermal chiller itself, that can be either an adsorption or absorption one, (iii) a component for heat rejection (e.g. a wet cooling tower or a dry cooler), (iv) a back-up system (either a gas heater connected to the hot storage or a vapour compression chiller), and (v) the cold distribution system to the user [4,37].

The main drawbacks of this layout are the high number of components, which increases the overall free volume needed, the complexity in the installation, and the difficulty in implementing a single control logic for the system.

On the contrary, the solution developed in the framework of ZEOSOL combines in a single unit a hybrid adsorption-compression chiller and the dry cooler. Moreover, the solution will include also the solar thermal collectors and a small storage tank as a single-package to define a simple, standardized and modular solution allowing for reduced size and wide cooling capacity installations (i.e. 10 kW to hundreds of kW). The overall layout of the system is shown in Fig. 1, where the main components and the auxiliaries are highlighted. The core of the system is the integrated hybrid unit, which comprises the adsorption chiller, vapour compression chiller, the dry cooler and the hydraulic system in a single component. All the electric connections and control logic are managed by a single controller installed in this unit as well. In the next sections, the experimental testing of the main components will be presented, whereas the sizing of the entire system, including the auxiliaries, will be discussed in section 4, presenting the simplified sizing tool and methodological approach applied.

3. Experimental

The main components of the proposed solar cooling system were firstly tested as stand-alone components, in order to get information on their achievable performance, to be subsequently employed in the definition of the control logic and as input data for the simplified sizing tool.

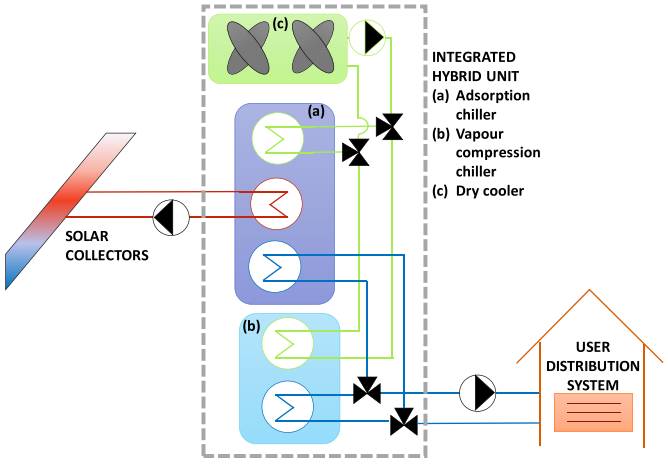

Fig. 1. Layout of ZEOSOL solution.

3.1. Solar thermal collectors

The solar collectors developed within the project are heat pipe evacuated tube collectors, able to provide heat to the hybrid module in a temperature range between 65 and 95 °C. Their main feature is the utilization of a single tube collector design. This solution presents some advantages over standard design of solar collectors [47,48] in terms of reduced manufacturing cost as well as installation cost and effort. Moreover, the possibility of forming plastics in different shapes allows for a tailored design, optimised for the reduction of pressure drop. Indeed, the efficiency of the solar collectors is a critical issue in solar cooling systems, as already been proven [8,10], since high thermal losses and poor heat transfer can limit the energy collected and therefore the heat available for the thermally driven chiller, resulting in the need for higher installed surfaces or heat integration. A general trend in the development of solar thermal collectors is the use of concentrators [48], but this complicates the installation effort needed and the costs, thus not representing an optimal choice for residential buildings. The solution proposed, instead, relies on the use of plastic materials and a simplified assembling method for the reduction of manufacturing and installation costs: single manifold elements can be added in a row until the desired performance is achieved or the available space is utilized. Indeed, since they are equipped with special end caps, the connection pipes to the storage tank only need to be clicked in. Fig. 2 shows the 3D view of the single-tube collector concept, while Fig. 3 shows the prototype collector with single tubes (STC) installed on the mounting frame.

The housing is made from fibre-reinforced plastic based on PPS (Polyphenylene sulphide). PPS is a semi crystalline, high temperature thermoplastic polymer. Due to its structure, PPS is a chemically resistant polymer with high mechanical strength, even at temperatures above 200 °C. In addition, it is especially interesting in solar applications thanks to its low water absorption, good dimensional stability, flame retardant properties and high weathering and radiation resistance [49]. Consequently, the resulting material has high thermal-mechanical strength, high hardness and stiffness, high dimensional stability and creep resistance, as well as good chemical resistance for a working temperature is up 260 °C. The insulating properties of such a materials are good, thus reducing the need for insulation. Nonetheless, to avoid heat losses, EPDM isolation material is mounted between the inner heat-conducting part and the outer shell.

Using injection-moulded plastic technology AkoTec was able to use new geometries to design the housing instead of copper or steel pipes that are used traditionally. In this way, it is possible to optimise the heat transfer from the heat-pipe vacuum tubes to the solar fluid, which, in turn, increases the performance of the thermally driven chiller. Within the design process, cost efficiency was considered: indeed, the plastic material used is expensive compared to other common plastics and requires heated moulds and high temperatures. However, the assembly production of the conventional collectors, that are made of steel, copper and insulating material, which are processed in many process steps, is drastically simplified, which allows an overall reduction of the costs.

Thanks to a coupled fluid dynamics and heat transfer study with finite elements methods, a geometry was realized, which is able to keep the flow of the solar fluid as turbulent as possible, without causing a high pressure loss. Specific tests were carried out at AkoTec to measure the pressure drop of the tubes in a dedicated testing rig, which is shown in Fig. 4. The results are reported in

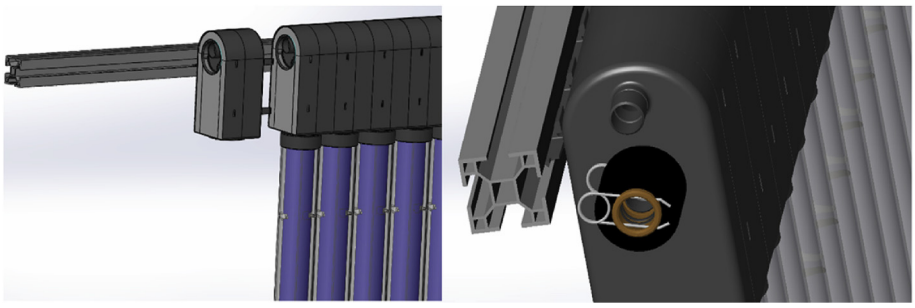

Fig. 2. 3D view of the single-tube collector concept with the plastic manifold module.

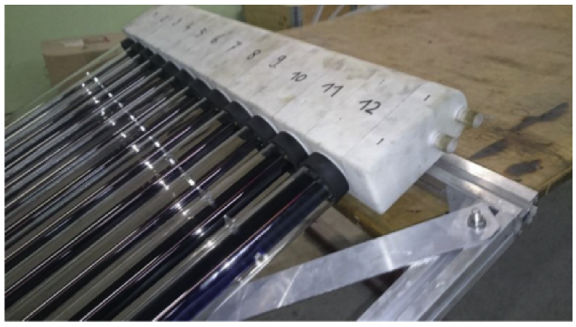

Fig. 3. STC-HP manifold unit with tubes on mounting frame.

Fig. 5 where standard AkoTec heat pipe evacuated tube collectors [50] are compared with the design developed: due to the reduced pressure drop of the new design, it is possible to reduce the pumping work or, keeping the same pressure drops as the standard design, it is possible to have 45% more heat with the same electrical consumption of the pumps.

Finally, the collectors were tested according to ISO 9806, in order to derive the characteristic coefficients for the calculation of solar performance and solar yield.

The performance of a solar collector can be expressed as [51]:

$$\frac{Q}{A} = G\left(\eta_0 - a_1\frac{T_{coll} - T_{amb}}{G} - a_2\frac{(T_{coll} - T_{amb})^2}{G}\right) \quad (1)$$

Where: Q is the heat gain from the collector, A is the aperture area of the collector, T_{coll} is the temperature of the absorber, T_{amb} is the ambient temperature, G is the solar irradiance, η_0 is the maximum optical efficiency of the collectors and a_1 and a_2 are the loss coefficients. The coefficients η_0, a_1 and a_2 were derived from the test report according to ISO 9806 conducted by a certified institute.

The results are reported in Table 1 and Fig. 6: a significant improvement of the η_0 value from 70 to 75.5% was measured compared to the standard AkoTec HP collector. This is attributed to the improved flow around the sleeves. The loss coefficients in the prototype were very high due to thermal bridges to the carrier frame, which can be significantly reduced in a future design.

The coefficients of Table 1 were used for the simulation of the annual solar yield in different locations implemented into the sizing tool.

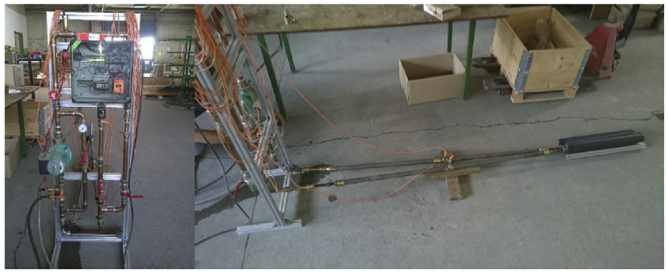

Fig. 4. The testing rig at AkoTec for the measurement of pressure drop in the STC.

3.2. The integrated hybrid unit

The core of the ZEOSOL solution is the integrated hybrid unit, which comprises a hybrid chiller and the dry cooler. In turn, the hybrid chiller combines a thermal (adsorption) chiller with an electric (vapour compression) unit in a single module, allowing the exploitation of the features and advantages of both systems [52]:

- The thermal chiller has a high electric efficiency, since it requires electricity only to drive the auxiliaries. It shows good performance in mild climate regions and can effectively exploit the solar renewable heat.
- The electric chiller allows having a precise temperature regulation and a fast response to load variations even under very high ambient temperatures. However, its electric efficiency is lower than the one of the thermal unit.

The main specifications of the adsorption unit and vapour compression unit tested and integrated are given in Table 2 and Table 3.

By combining of the two technologies, it is possible to cover the peak loads, reducing the number of solar collectors and capacity of the adsorption chiller unit, providing an excellent part-load operation at the same time. However, for the full exploitation of the potentiality of the hybrid unit, it is necessary to define a proper control strategy, defining the conditions under which the thermal and electric chiller can run in parallel or only a single unit (either thermal or electric) must be turned on. To this aim, an extensive experimental campaign was carried out separately with the two units. The results are then integrated into the sizing tool.

3.3. Experimental facilities

3.3.1. Testing facilities for adsorption unit

In order to characterize the performance of the adsorption module of the ZEOSOL system, experiments have been carried out in a testing rig located at Fahrenheit GmbH, able to supply a constant inlet temperature for the high, medium and low temperature loops. The schematic of the testing rig is shown in Fig. 7. The hot water for the desorption step (HT) is provided via a water reservoir, which is connected to a boiler. This allows a constant driving temperature of up to 95 °C. The medium temperature circuit (MT)

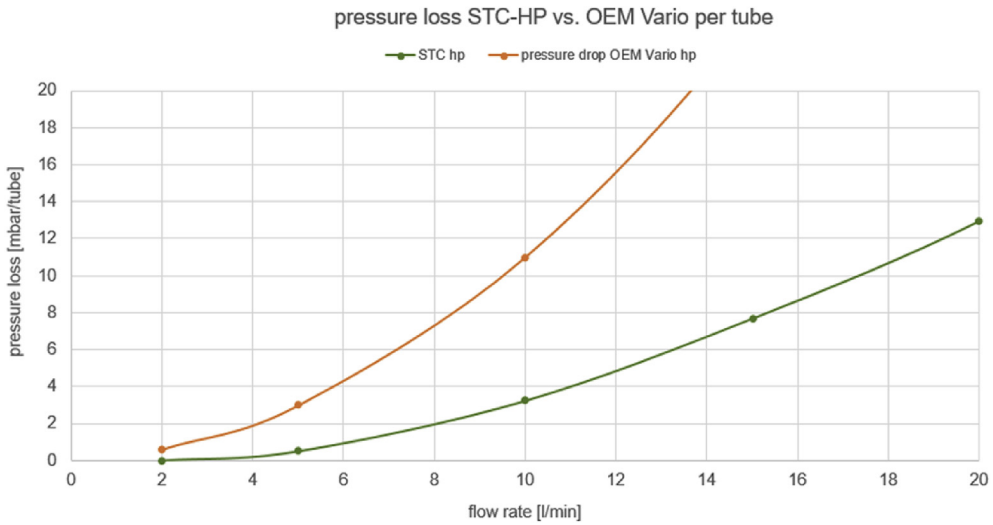

Fig. 5. Results of pressure drop tests at AkoTec.

Table 1
Performance of the solar collector developed in comparison with the standard AkoTec product.

Collector type	η_0	a_1	a_2	G
	–	W/(m2K)	W/(m^{2}K^2)	W/m^2
OEM Vario HP	0.703	2.224	0.005	970
STC HP ZEOSOL	0.755	2.560	0.0081	

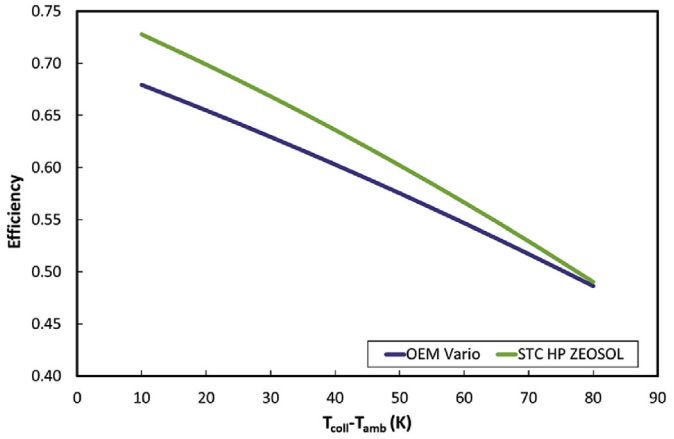

Fig. 6. Efficiency of the developed solar collectors in comparison with the standard AkoTec product.

Table 2
Specifications of the adsorption unit.

Parameter	Unit	Value
Dimensions W x D x H	mm	875 × 765 × 2004 mm
Weight	kg	370
Nominal cooling capacity	kW	16.7
Nominal COP	–	0.65
Maximum power consumption	kW	0.80
Nominal power consumption	kW	0.26
Chilled water circuit – nominal volume flow	kg/min	42
Cooling water circuit – nominal volume flow	kg/min	85
Hot water circuit – nominal volume flow	kg/min	48

Table 3
Specifications of the vapour compression unit.

Parameter	Unit	Value
Dimensions W x D x H	mm	850 × 1500 × 2000
Weight	kg	300
Nominal cooling capacity	kW	31
Maximum power consumption	kW	12
Nominal power consumption	kW	9.2
Compressor type	–	scroll
Refrigerant	–	R134a
Chilled water circuit – maximum volume flow	kg/min	89
Cooling water circuit – maximum volume flow	kg/min	103

and the low temperature circuit (LT) are regulated by means of plate heat exchangers and motorised valves regulating the inlet temperature: the primary circuit of the heat exchangers is connected to a water reservoir and a circuit with a throttle to control the temperature, whereas the secondary circuit is connected to the correspondent hydraulic loop of the adsorption unit. All the circuits are supplied with pumps to control the flow. The control and recording of the measurement data is realized via the software LabVIEW that also allows automatic management of temperature set-points, closing and opening of throttles and control of the volume flows. The sensors used are listed in Table 4.

3.3.2. *Testing facilities for vapour compression chiller and dry-cooler units*

The vapour compression chiller and the dry cooler were tested in the labs of CENTROPROVE at CNR-ITAE. The testing rig used for the purpose, which was designed for the experimental characterization of thermal and hybrid units is described in Ref. [22] and mainly consists of a gas heater and an electric chiller. The gas heater is used to heat up a hot water storage of 1.5 m^3, whereas the electric chiller cools down a 1 m^3 water storage. The desired temperature level in each circuit is achieved by mixing the water of these storages through 3-way mixing valves and thermostats. A picture of the testing rig is shown in Fig. 8. The sensors installed and their accuracy are reported in Table 5.

3.4. *Adsorption unit: test results*

Aim of the tests of the adsorption chiller was the definition of a

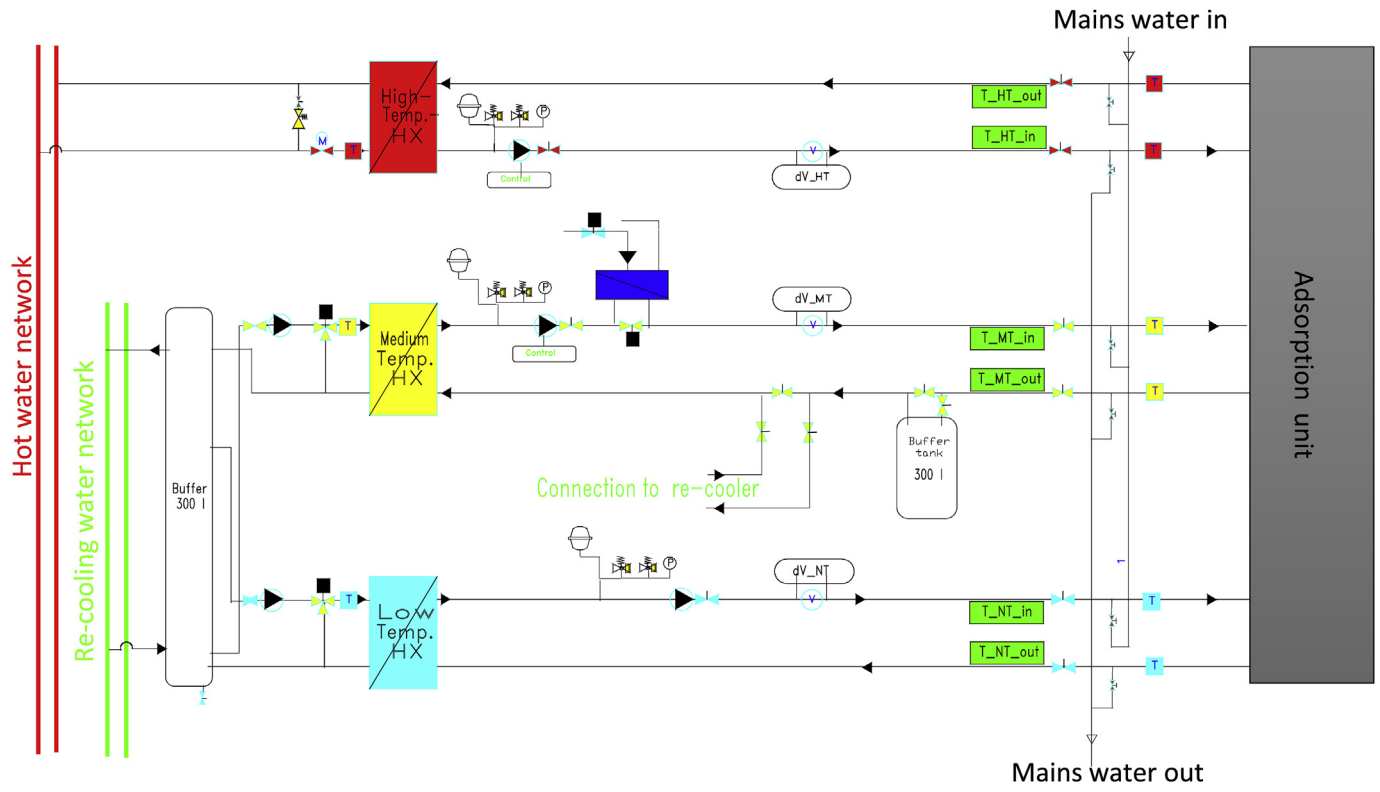

Fig. 7. The testing facility at Fahrenheit Gmbh used for the testing of the adsorption unit.

Table 4
Sensors installed in the testing rig at Fahrenheit.

Sensor	Model	Class/Accuracy	Parameter measured
RTD	Pt100	1/3 DIN	Temperatures of the inlet/outlet circuits of the tested unit (example T_HT_out)
Magnetic inductive flow meters	VMM25	±0,5% FS	Flow rate in HT- and LT-circuits.
Magnetic inductive flow meters	VMM32	±0,5% FS	Flow rate in MT-circuit

map of performance of the unit, in terms of cooling capacity, thermal COP, and electricity consumption as a function of the operating temperatures (i.e. heat source, condensation and evaporation temperatures). In particular, the following ranges were tested:

Fig. 8. The testing rig at CNR-ITAE.

- HT_{in}: 65–95 °C
- MT_{in}: 25–40 °C
- LT_{in}: 19 °C, LT_{out}: 16 °C

Nominal flow rates were selected in all circuits. The following parameters were calculated:

- cooling capacity:

$$\dot{Q}_{LT} = \dot{m}_{LT} c_p (T_{LT,in} - T_{LT,out}) \quad (2)$$

- thermal COP, defined as the ratio between the cooling capacity $\dot{Q}_{LT}$ and the heat supplied $\dot{Q}_{HT}$:

$$COP_{th} = \frac{\dot{Q}_{LT}}{\dot{Q}_{HT}} \quad (3)$$

- EER (Energy Efficiency Ratio), defined as the ratio between the cooling capacity $\dot{Q}_{LT}$ and the electric power consumption E_{el}:

$$EER = \frac{\dot{Q}_{LT}}{E_{el}} \quad (4)$$

Table 5
Sensors installed in the testing rig at CNR ITAE.

Sensor	Model	Class/Accuracy	Parameter measured
Thermocouple	Type-T	Class 1	Temperatures of inlet/outlet circuits of the testing rig and the storages
RTD	Pt100	1/3 DIN	Temperatures of the inlet/outlet circuits of the unit tested.
Magnetic flow meters	MVM250-PA	±2.5% FS	Flow rate in all circuits.
Electric energy meter	Sineax DM5S	Class A o ICES-0003.	Voltage, current, frequency, active and reactive power of the aggregate.

The results are reported, for the most interesting operating conditions, in Fig. 9 (cooling capacity), Fig. 10 (thermal COP) and Fig. 11 (EER). As widely proven, the cooling capacity and thermal COP reduce with increasing condensation temperature and with a reduced heat source temperature [22], which, in turn, results in a decrease of the EER of the unit. It is worth pointing out that, already at 32 °C condensation temperature, the cooling capacity that the unit can deliver drops to 65% of the nominal one (at 95 °C heat source temperature) or even lower (25% of the nominal one at 65 °C heat source temperature), thus already giving useful indication for the future definition of the management strategy, i.e. at condensation temperatures higher than this one, the use of compression chiller is mandatory to cover the peak load.

Nonetheless, as pointed out in section 3.2, the main advantages of using the hybrid configuration is that the EER of the adsorption unit is very high and thus allows for a reduced electricity consumption. Indeed, as shown in Fig. 12, when the heat source temperature is 85 °C, the EER of the system ranges from 47 to 34, passing from 25 °C to 32 °C. Even at lower heat source temperatures, i.e. 65 °C, while still getting cooling capacities ranging from 12 kW to 4 kW, the EER ranges from 35 to 17, indicating substantial electricity consumption savings.

Finally, the thermal COP of the unit is always in the range 0.6 to 0.4 under the investigated conditions, which is quite close to the theoretical values achievable, and thus denoting a good design [9].

The performance maps reported were then used as input data for the sizing tool developed.

3.5. Vapour compression chiller: test results

Aim of the tests of the vapour compression chiller was the definition of a map of performance of the unit, based on the cooling capacity and electricity consumption as a function of the operating temperatures (i.e. in the evaporator and condenser circuit) and design parameters (i.e. flow rates in the circuits). In order to better understand the trends of all the parameters monitored and recorded and to give an overview of the measured data, the graphs of typical base tests are shown in Figs. 12–14.

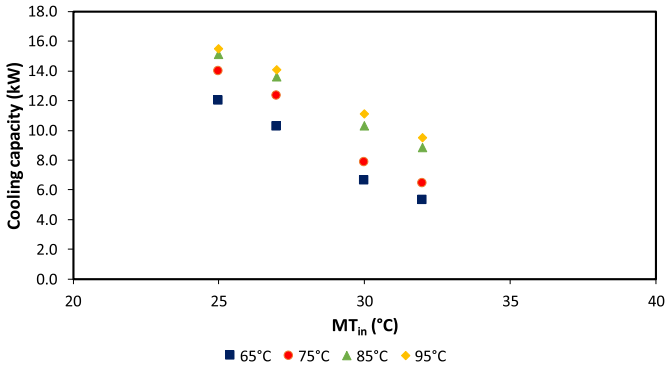

Fig. 9. Cooling power of the adsorption unit as a function of condensation (MT_{in}) and heat source temperatures.

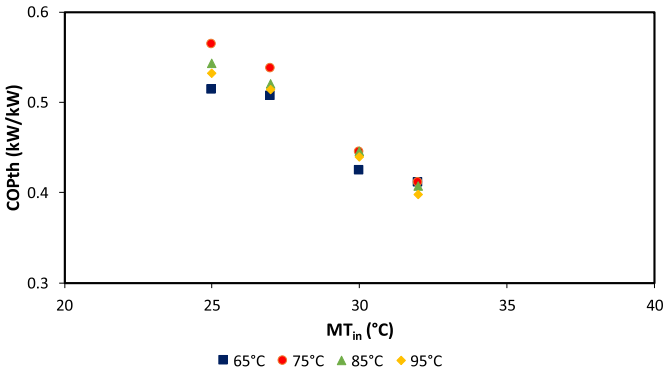

Fig. 10. Thermal COP of the adsorption unit as a function of condensation and heat source temperatures.

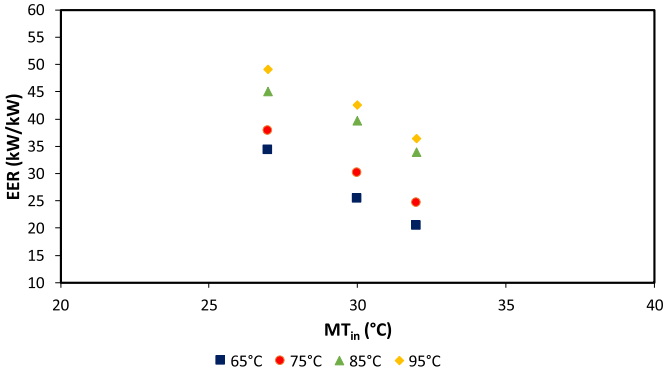

Fig. 11. EER of the adsorption unit as a function of condensation and heat source temperatures.

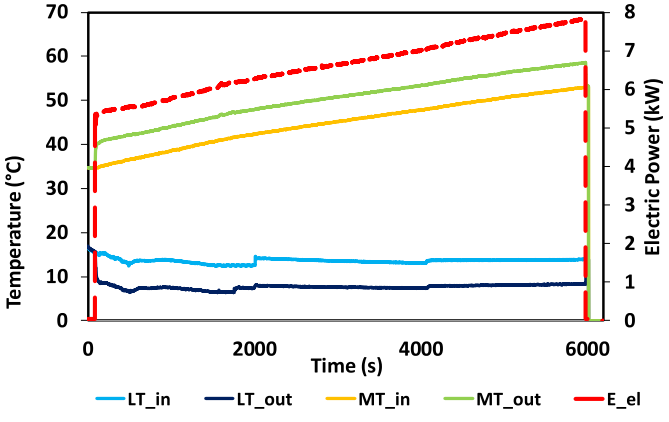

Fig. 12. Typical base test: Temperatures and electric power consumption. (LT_{set} 7 °C; LT and MT flow rate 45 kg/min).

The test procedure selected is as follows:

- The chilled water set-point temperature (LT_{set}) is defined;
- The flow rates in the MT (condenser) and LT (evaporator) circuits are defined and set to a constant value;
- A temperature ramp is set in the electronic controlling unit of the mixing valve for the MT circuit, varying the inlet to the condenser circuit between 25 °C and 60 °C, corresponding to the operating limits for the tested chiller.

The parameters recorded include the temperatures, the electric power consumption, and the flow rates. In addition, the following parameters are calculated:

- cooling capacity, according to Equation (2);
- EER (Energy Efficiency Ratio), defined as the ratio between the cooling capacity $\dot{Q}_{LT}$ and the electric power consumption E_{el}, according to Equation (4).

Figs. 12 and 13 show the temperatures and the electric power consumption for two different flow rates, 45 kg/min (nominal flow rate) and 22 kg/min, respectively. It can be observed that, for the nominal flow rate (Fig. 12), the difference between the inlet and the outlet of the MT and LT circuits is around 5 K, corresponding to the design values. For the tests with reduced flow rate (Fig. 13) the temperature difference between the inlet and outlet in the MT and LT loops increases (up to 18 K in the MT loop). Consequently, the maximum condenser inlet temperature allowed is lower than in the previous case (35 °C against 50 °C).

Fig. 14 shows the cooling capacity and electric power consumption with increasing time (and hence temperature MT_{in}), for each test separately (see (a), (b)) and in a direct comparison (c). It is possible to notice that the lower flow rates guarantees a lower power consumption, with savings up to 25%, without hindering the cooling power that the chiller can provide. However, as already stated, the operating limit is reached at a lower temperature. These results indicate that, by adjusting the flow rate of the pumps, it is possible to optimise the operation of the chiller even if this is not equipped with a variable speed compressor and to switch to nominal flow rate once the outlet temperature approximates the limit one.

Finally, the results measured were aggregated in order to create a performance map of the electric chiller to be used for sizing purposes. The cooling capacity and EER were derived as a function of the temperature lift ($MT_{in} - LT_{out}$), as shown in Fig. 15. A clear general trend can be observed: the cooling capacity and EER reduce for higher values of the temperature lift, corresponding to the very severe operating conditions. However, it should be mentioned that the unit tested is capable to produce up to 31 kW of cooling capacity for the lower external temperature and it still can produce 15 kW of cold with very high external temperature (44 °C). The measured EER also reaches very high values: it ranges from 7.8 to 2.2.

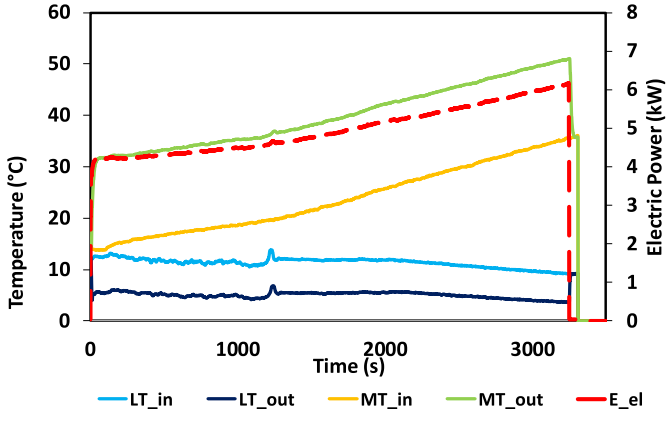

Fig. 13. Typical base test: Temperatures and electric power consumption (LT_{set} 5 °C; LT and MT flow rate 22 kg/min).

3.5.1. Dry cooler unit: test results

The dry cooler unit selected for the ZEOSOL system is a V-shaped commercial unit, whose specifications were chosen considering the installation in hot climates. The main features of the dry cooler are reported in Table 6.

Aim of the tests of the dry cooler was the definition of a map of performance of the unit, indicating the cooling capacity, pressure drop and electricity consumption as a function of the operating temperatures (i.e. difference between the inlet temperature and the ambient temperature) and design parameters (i.e. flow rates in the circuits and speed of the fans).

Accordingly, two type of tests were performed:

1. Evaluation of the effect of the water flow rate: the speed of the fans was set to the maximum value, which corresponds to an analogue signal input tension of 10 V, while the water flow rate was varied from 60 kg/min to 20 kg/min;
2. Evaluation of effect of the speed of the fans: the water flow rate was kept at 60 kg/min and the speed of the fans was varied from 100% to 20% by varying the analogue input tension to the unit from 10 V to 2 V.

The results of the first series of tests are reported in Fig. 16, where the cooling power is plotted as a function of the temperature difference between the water inlet temperature (DC_{in}) and ambient air temperature (T_{amb}). The results clearly show that the cooling capacity decreases both when reducing the water flow rate and the temperature. However, it is worth noticing that a very wide range of conditions was evaluated, with the aim of defining a reliable interpolation of experimental data for the implementation of the sizing tool. Design conditions, instead, are those highlighted in the yellow area. For the specific case of $\Delta T = 5$ K, the cooling power of the dry cooler is 12 kW for a flow rate of 60 kg/min, 10 kW for a flow rate of 40 kg/min and 7 kW for a flow rate of 20 kg/min. Consequently, reducing the flow rate does not prove an effective measure and all the other tests were carried out with a flow rate of 60 kg/min on the water side. In addition, the pressure drop with the varying flow rate was measured, which ranges from 170 mbar to 30 mbar for a water flow rate of 60 kg/min and 20 kg/min, respectively.

The results of the second series of tests are shown in Fig. 17a, where the cooling power is plotted against the ΔT between inlet of the dry cooler and ambient temperature, as a function of the speed of the fans. It shows that reducing the speed of the fans to 20% of the maximum value actually reduces the cooling power of the chiller. Instead, the difference between the other conditions seem negligible (i.e. < 15%) for most conditions. However, to better highlight the effect of such a parameter in design conditions, a detail on the cooling power at low ΔT is shown in Fig. 17b: considering a ΔT of 5 °C, the measured cooling power is 12 kW with the fans at maximum velocity (10 V) and 7 kW with the fans at minimum velocity (2 V). It is interesting to point out that the tendency shown is linear: the power of the dry cooler (at least in design conditions) increases linearly with the ΔT. This result was used in the definition of the sizing tool, by considering that the speed of the fans can be modulated according to the cooling capacity needed.

Finally, the electricity consumption as a function of the fans'

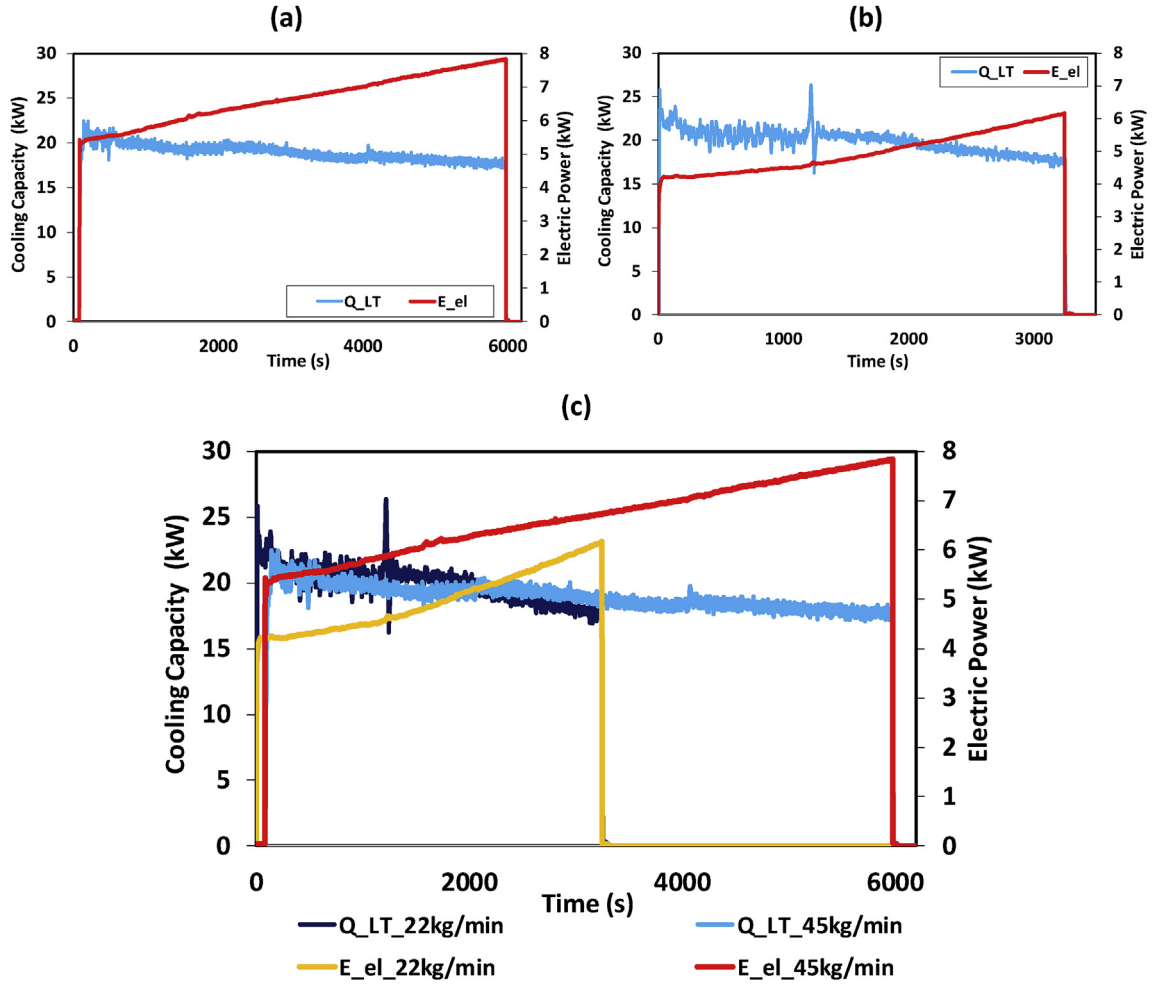

Fig. 14. Typical base test: cooling capacity and electric power consumption: (a) LT_{set} 7 °C; LT and MT flow rate 45 kg/min; (b) LT_{set} 5 °C; LT and MT flow rate 22 kg/min; (c) comparison of both cases.

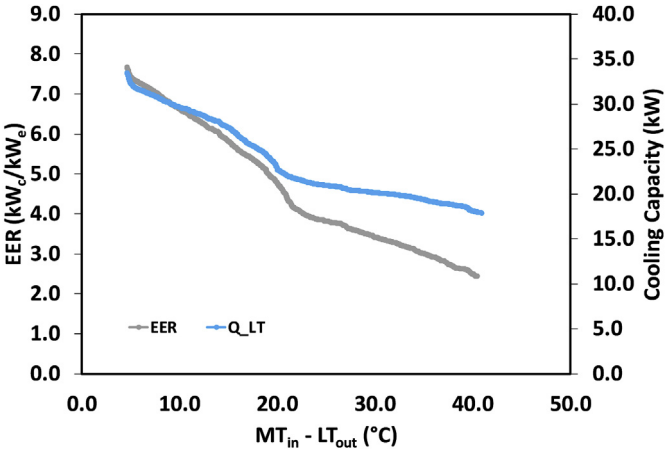

Fig. 15. Map of performance of the vapour compression chiller.

speed was also evaluated, as shown in Fig. 18: the power needed for the operation of the dry cooler depends on the square of the speed of the fans, which further stresses the importance of modulating the speed of the fans for a proper optimization of the system.

Table 6
Specifications of the dry cooler unit.

Parameter	Unit	Value
Dimensions W x D x H	mm	2755 × 1180 × 1700
Weight	kg	441
Nominal capacity	kW	37.5
Design conditions (water)	°C	In: 42– Out: 37
Maximum water volume flow	kg/min	108
Design conditions (air)	°C	In: 35 – Out: 38.8
Maximum air volume flow	m^3/h	In: 30445 – Out: 30881
Maximum power consumption	kW	0.87

4. Design guidelines and the simplified sizing tool

4.1. Generalities

Usually, the sizing of a solar cooling system is accomplished using dynamic modelling tools, able to follow the variation of the sun and therefore of the solar yield. A typical example, as already reported in the literature analysis, is the use of TRNSYS. However, this approach has two main drawbacks: (i) TRNSYS is a proprietary software, whereas a sizing tool for a commercial system should be made available to a vast audience of designers and users; (ii) the use of these tools is far from intuitive and requires a learning curve and time to set up a model each time an evaluation is needed. On the

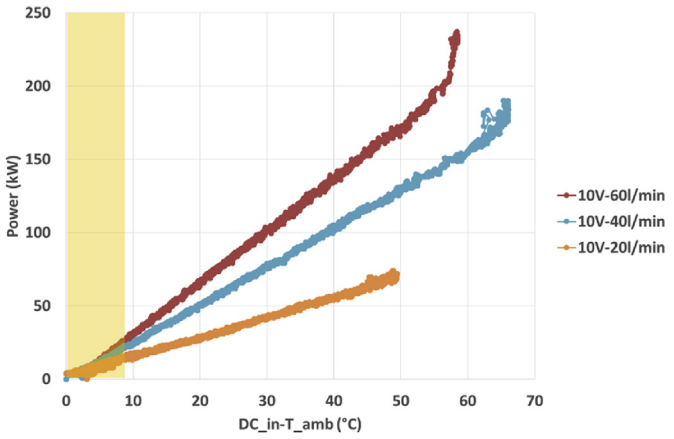

Fig. 16. Map of performance of the Dry Cooler at different flow rates of the water.

contrary, the vast diffusion of solar cooling systems requires a standard design *modus operandi* to be extended to situations even significantly different and should not be computationally complex despite being able to run on annual basis. Eventually, such a tool must be user-friendly. For this purpose, a simplified sizing tool was developed, that allows a simple evaluation of the system, based on the internal "AdCalc" tool by Fahrenheit. It allows adapting the calculation procedure to a wide range of conditions, simply by knowing the weather data, the specifications of the chillers and the solar collectors and the load to be met. Indeed, one of the advantages of the solution proposed, both in terms of design and installation is the modularity that actually poses no limitation to the potentiality of the tool introduced here. This means that, once the components to be used in the system are fixed, the methodology implemented can be easily re-used for the definition of standard sizing procedures, thus simplifying the design of the systems, which, in view of a massive commercialization, represents a significant achievement.

4.2. Methodological approach: a guide to design solar cooling systems

The methodology used in the sizing tool is schematically reported in Fig. 19, which can be considered a reference standard approach for the design of solar cooling systems.

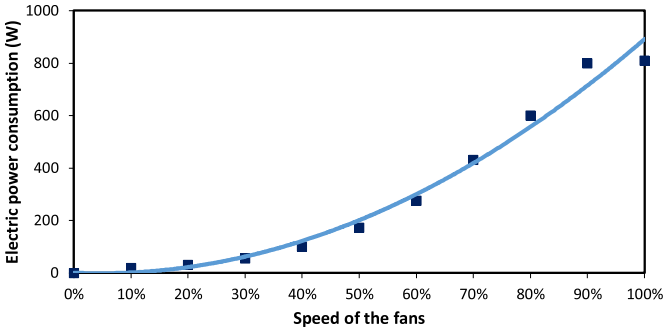

Fig. 18. Electric consumption of dry cooler at different fans velocities.

1. **The main input data is inserted into the tool.** It includes the weather data (solar irradiation, humidity and ambient temperature) as hourly values, obtained through Meteonorm or similar tools, the performance maps of the adsorption and vapour compression units, as defined in sections 3.4 and 3.5, respectively, as well as the characteristic equations of solar collectors (Equation (1) of section 3.1).
2. **The auxiliaries are sized.** As noted in the previous sections, the test results show clearly that by varying the flow rate of the pumps and the speed of the fans of the dry cooler the effect of auxiliaries on the overall electricity consumption of the system can be optimised. To this aim, a standardized procedure was applied, that assumes a linear dependency between the load to be met and the variation of the speed of the fans and the flow rate of the pumps, respectively. To define the correct correlation, the data taken from the datasheet of the pumps installed in the unit were interpolated as a function of flow rate, as shown in Fig. 20.

The following equations were used:

$$E_{HT\_pump}[W] = \begin{cases} 57.5\dot{m} + 30.833 & \dot{m} < 2\left[m^3h^{-1}\right] \\ 150 & \dot{m} \geq 2\left[m^3h^{-1}\right] \end{cases} \quad (5)$$

$$E_{MT\_pump}[W] = 0.9238\dot{m}^2 + 34.357\dot{m} - 1.3095 \quad (6)$$

$$E_{LT\_pump}[W] = -1.346\dot{m}^2 + 46.328\dot{m} + 1.9697 \quad (7)$$

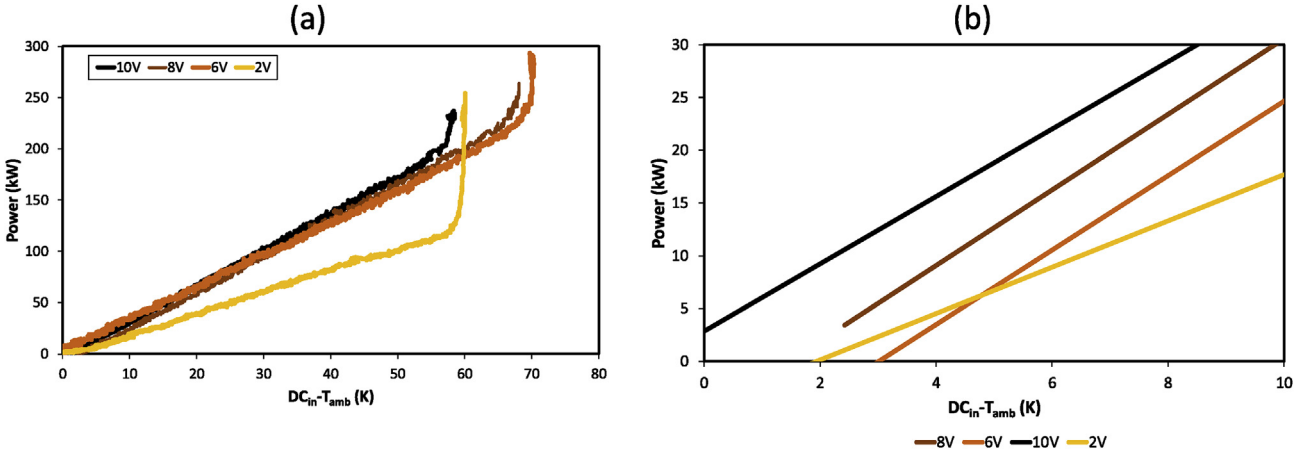

Fig. 17. Map of performance of the Dry Cooler at different speed of the fans: (a) overall conditions investigated; (b) design conditions.

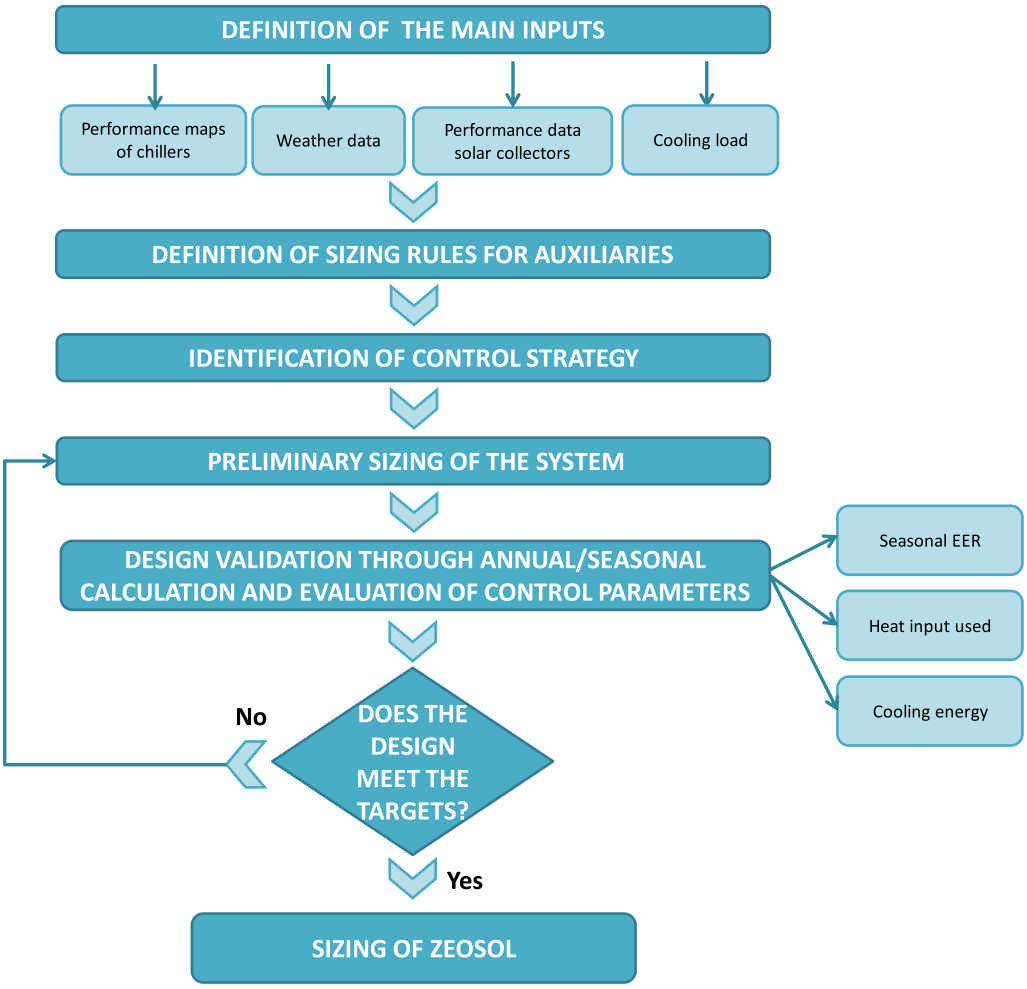

Fig. 19. Methodology flow-chart for simplified design of ZEOSOL.

Subsequently, the proper flow rate under each condition (part load ratio f) was calculated assuming that, for 100% part load ratio, the flow rate corresponds to the nominal one declared by the chiller producers.

Consequently, the optimal flow rate in each circuit for a specific load is given by:

$$\dot{m}(f) = \frac{\dot{m}_{nominal}}{\dot{Q}_{nominal}} \dot{Q}_{actual}(f) \tag{8}$$

The values of $\gamma = \frac{\dot{m}_{nominal}}{\dot{Q}_{nominal}}$ for each pump are reported in Table 7.

In addition, the consumption of the dry-cooler was considered, in accordance with experimental data introduced in the previous section. The following equation was used, which fits the data reported in the chart of Fig. 20:

$$E_{DC} = 979.55v^2 - 88.536v + 0.7 \tag{9}$$

Where v is the speed of the fans in percentage over the maximum value.

3. **The control strategy is identified.** For the hybrid system examined, four operating modes are possible. The decision process for the identification of the operating mode as a function of operating conditions and control parameters is reported in Fig. 21. It can be summarized as follows:
   - **Free Cooling:** In case the dry cooler unit can supply enough cooling to fulfil the cooling need, with low outdoor temperatures, the ZEOSOL system is working in free cooling mode.
   - **Adsorption cooling:** If free cooling is not possible and there is heat available to drive the adsorption system at an EER higher than the one of the compression unit of the ZEOSOL system, the adsorption unit delivers the cooling needed.
   - **Bivalent cooling:** In case the cooling load cannot be met by adsorption cooling, the compression unit delivers the rest of the cooling power needed. The adsorption and the compression part of the ZEOSOL system run in parallel.
   - **Compression cooling:** If free cooling is not possible and there is no heat from the solar collectors available to drive the adsorption part of the ZEOSOL system, the cooling need is fulfilled only by compression cooling. The same is the case if the conditions are such that the solar heat can only be used to drive the adsorption system with a high amount of energy for re-cooling and pumps and thus at a lower EER than the compression unit.
4. **A preliminary sizing of the system is defined**, in terms of nominal cooling capacities of the adsorption and the compression units, and surface of solar field.
5. **The design is validated.** The parameters used for the evaluation of the design are strongly dependent from each specific case, but it can be assumed that the seasonal EER and the solar fraction of the system represent a good choice for the estimation of the benefits achievable under a wide range of conditions. Design

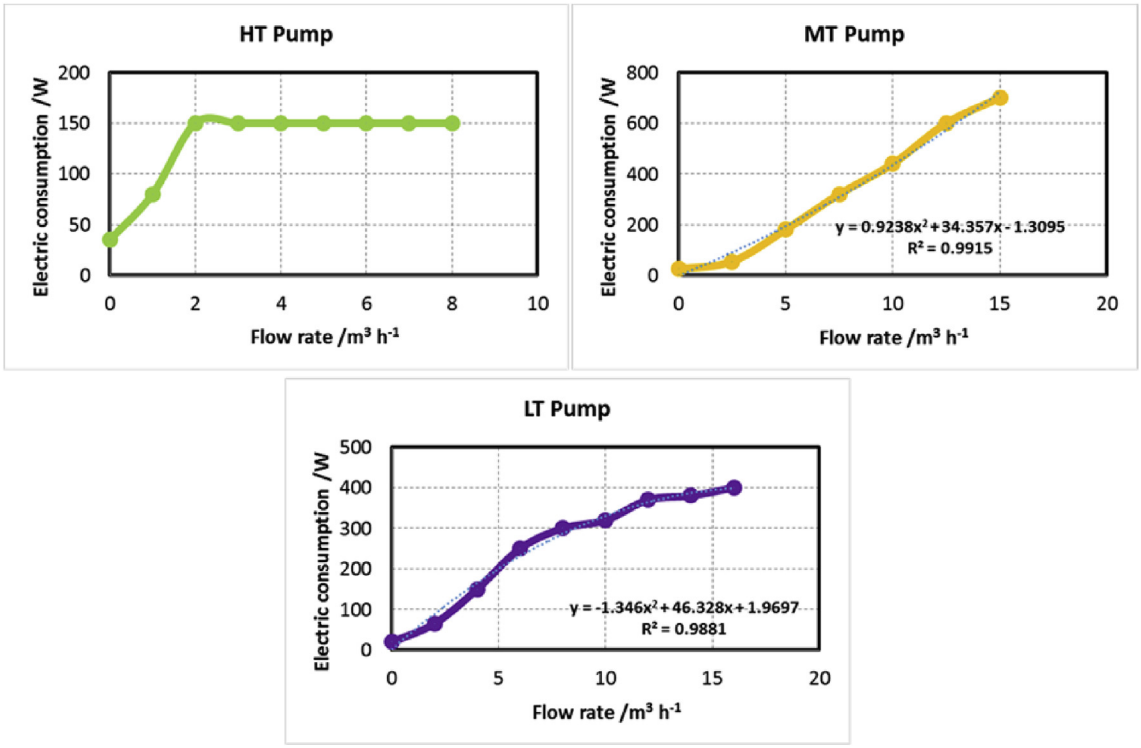

Fig. 20. Electric consumption of the pumps in the hybrid unit as a function of flow rate.

Table 7
γ of the various pumps.

Pump	γ[kg h^{-1}/kW]
HT	100
MT	94.5
LT	254.2

validation is obtained through a calculation for the cooling season (that corresponds to annual conditions in severely warm climates, such as in Middle East and Arab countries).

6. **The final design is obtained** through iteration of the design evaluation until the desired targets are reached.

4.3. Tool validation and comparison with different solutions

Real installations – or even lab-scale measurement – on hybrid adsorption/compression systems are still limited, since the majority of studies focus on absorption/compression combined cycles, as reported in Ref. [52]. Nonetheless, an attempt was made at validating both the proposed configuration and the sizing tool itself. In particular, the EER of the ZEOSOL system was compared to: (a) the first version of the commercial hybrid chiller put on the market by Sortech in 2017 and tested in the laboratories of CNR ITAE; (b) the cascade system tested at ITAE and whose results are published in Ref. [52]. The comparison is reported in Fig. 22: it is possible to notice that the EER of ZEOSOL simulated solution and the commercial system are quite similar, with the results of the ZEOSOL

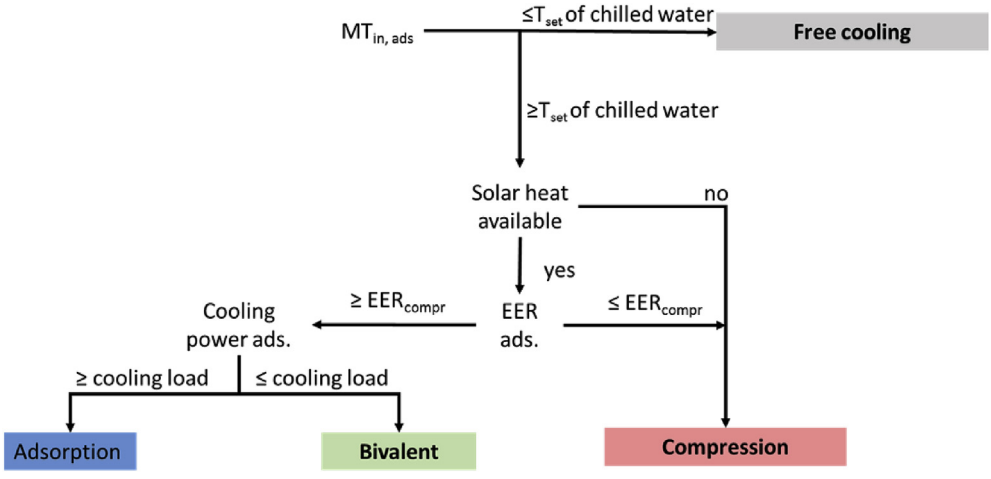

Fig. 21. Schematic of operation modes of the ZEOSOL system.

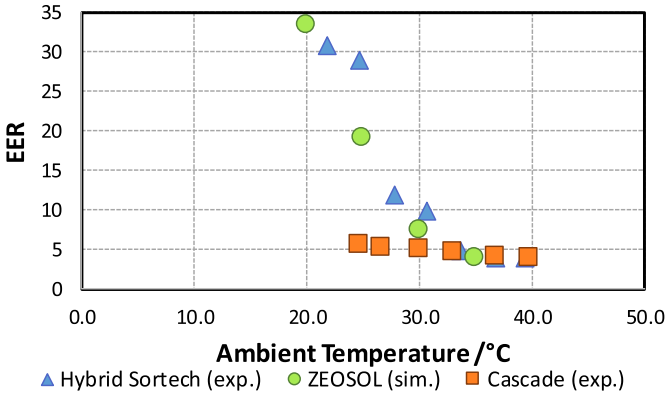

Fig. 22. Comparison of ZEOSOL solution with other hybrid adsorption-compression systems.

proposed system slightly higher, thanks to the improvement described above. Instead, for the application in solar cooling systems in residential buildings, the cascade solution is not competitive: since the operation of the adsorption chiller only is not possible, the EER at the lower ambient temperature is penalised, with a detrimental effect on the overall performance. Such results indicate not only that the developed tool is reliable and suitable for the design of such systems, but also that the proposed system has the potentiality to reach the targeted performance (ESEER of 15).

4.4. Case studies: results

The simplified sizing tool developed was applied to three case studies, corresponding to different locations and climates, namely Berlin, Athens, and Riyadh.

It is worth mentioning that the sizing tool is based on experimentally measured performance data for all the components (adsorption and compression chillers and auxiliaries such as dry cooler and pumps), thus guaranteeing a reliable output. A similar approach is often followed in other simulation tools, i.e. TRNSYS types 911 and 666 (adsorption and compression chiller, respectively) that make use of lookup tables. Furthermore, the tool will be validated in the final phase of the project with data gained from the monitoring of the pilot plant installation.

For all the locations, the same building and system layout were considered. In particular, the building is a class A+ house, whose main features are described in Ref. [35]. The configuration of the solar cooling system includes a solar field of 40 m^2 in combination with a 1000 L hot water tank corresponding to a specific storage ratio of 25 l/m^2: It has been already demonstrated that larger storage volumes do not affect the performance of solar cooling systems significantly [42]. A preliminary simulation was carried out in TRNSYS, using Meteonorm data of the chosen locations, in order to define the available solar heat, as well as the heating and cooling demand of the building. The main results of the simulations are reported in Table 8. Due to the different climates, both the solar energy that can be harvested from the solar field and the demand for space cooling and heating differ significantly.

Using these input data, a simulation of the ZEOSOL system performance was carried out (January–December) with the simplified tool. The main results, presented in Fig. 23, can be summarized as follows:

- Adsorption only mode is possible in Berlin and Athens.
- Bivalent mode occurs in all locations.
- The percentage of the cooling load covered by adsorption is similar in Berlin (47%) and Athens (41%), dropping to 12% in Riyadh.

Fig. 24 depicts the heat available from the solar field and the amount that is used for cooling. For all the examined cases, the heat

Table 8
Results of preliminary simulations in the three locations chosen for the application of the simplified sizing tool.

Parameter		Berlin	Athens	Riyadh
Outdoor air temperature	°C	−12.0 … 32.6	1.1 … 38.3	4.2 … 46.0
Cooling demand	kWh/year	3800	24,064	93,840
Cooling hours	h/year	937	3399	8519
Heat from solar energy @ >85 °C	kWh/year	18,544	49,266	86,237
Cooling hours with solar heat available	h/year	1383	2498	3404

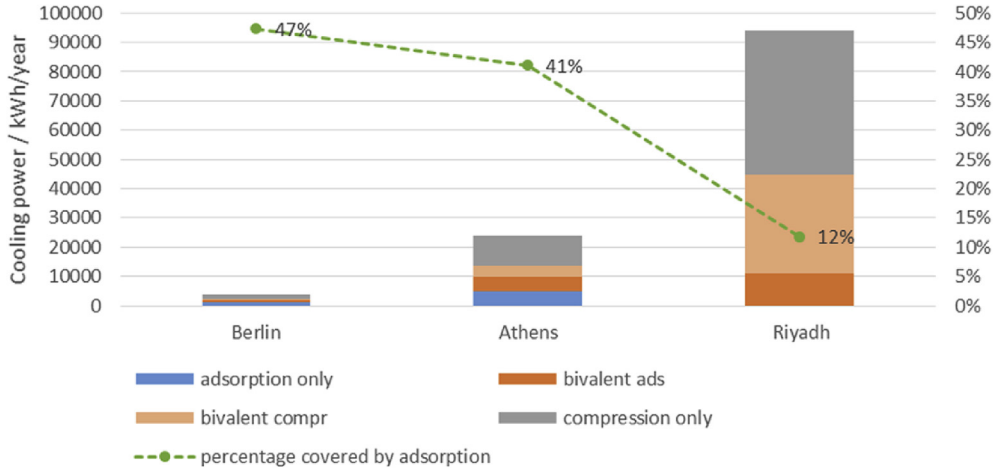

Fig. 23. Relevance of operation mode for different location: cooling power provided.

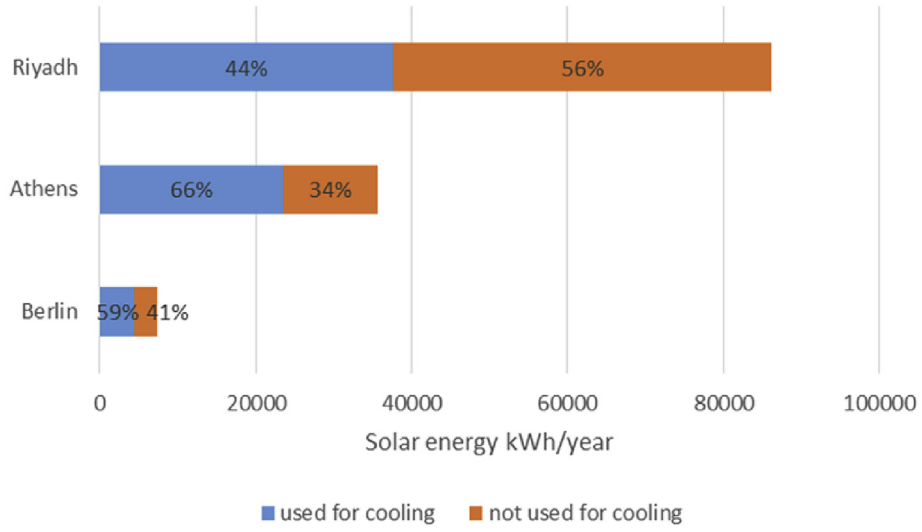

Fig. 24. Use of solar energy for adsorption cooling.

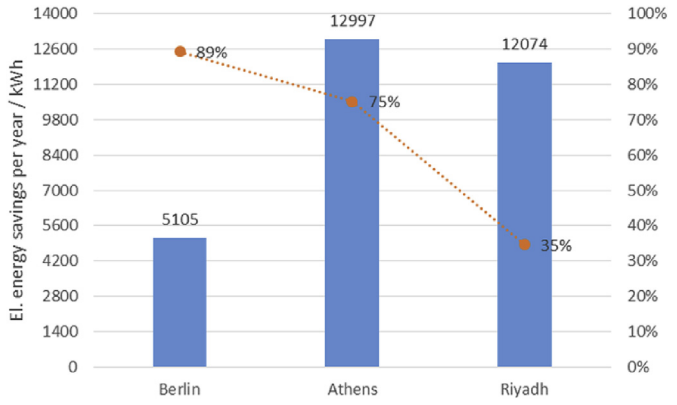

Fig. 25. Energy savings per year by the use of solar driven hybrid chiller for different locations.

available exceeds that one needed to drive the hybrid chiller, thus proving that the sizing of the system is correct. However, in Athens, most solar energy is used, only 34% is not used to produce cold, compared to 56% in Riyadh. This is due to the more severe ambient temperatures: for very high outdoor temperature the adsorption unit is not operated, as the electric unit EER is higher.

To further stress the useful information that can be extracted from the evaluation of data output from the sizing tool, the annual energy savings of the solar cooling system are calculated. The reference system used for comparison is the vapour compression chiller tested within the project. The results are shown in Fig. 25: energy savings up to 89% can be achieved in Berlin, where the cooling demand is limited and the lower outdoor temperature results in a higher efficiency of the adsorption part of the hybrid. Nonetheless, even in a hot climate, such as Athens, energy savings up to 75% were calculated, further stressing the benefit of solar cooling systems in these climates. In Riyadh, where the efficient operation of the adsorption unit is strongly hindered by the high condensation temperatures, 35% energy savings could still be achieved.

5. Conclusions

The present paper reports the experience and findings of the H2020 project ZEOSOL, whose aim is the development of an advanced solar cooling system, including an integrated hybrid chiller-dry cooler unit and efficient heat pipe evacuated tube solar collectors, all integrated with an optimised control strategy. The experimental activity on the different components is reported, which leads to the definition of their performance maps: the cooling capacity, thermal COP and EER of the adsorption chiller as a function of operating temperatures; the cooling capacity and EER of the vapour compression chiller as a function of operating temperatures. In addition, the experimental characterization of the dry cooler was carried out, defining the optimal operating point for each ambient temperature conditions.

Starting from such data, a simplified sizing methodology that can serve as guideline for the design of solar cooling systems in a wide variety of climates was developed and the results are presented for three cases: Berlin, Athens and Riyadh. The results validated the sizing process applied and allowed for the calculation of annual energy savings, which range from 35% in Riyadh to 89% in Berlin, further proving the benefit of replacing traditional space cooling systems with solar-powered ones.

Acknowledgments

This project has received funding from the EUROPEAN COMMISSION, Executive Agency for Small and Medium-sized Enterprises, Grant Agreement number: 760210 — ZEOSOL — H2020-FTIPilot-2016/H2020-FTIPilot-2016-1.

References

[1] R.M. Lazzarin, M. Noro, Past, present, future of solar cooling: technical and economical considerations, Sol. Energy 172 (2018) 2–13, https://doi.org/10.1016/J.SOLENER.2017.12.055.
[2] F.M. Montagnino, Solar cooling technologies. Design, application and performance of existing projects, Sol. Energy 154 (2017) 144–157, https://doi.org/10.1016/J.SOLENER.2017.01.033.
[3] J. Settino, T. Sant, C. Micallef, M. Farrugia, C. Spiteri Staines, J. Licari, A. Micallef, Overview of solar technologies for electricity, heating and cooling production, Renew. Sustain. Energy Rev. 90 (2018) 892–909, https://doi.org/10.1016/J.RSER.2018.03.112.
[4] U. Eicker, D. Pietruschka, M. Haag, A. Schmitt, Systematic design and analysis of solar thermal cooling systems in different climates, Renew. Energy 80 (2015) 827–836, https://doi.org/10.1016/J.RENENE.2015.02.019.
[5] U. Eicker, E. Demir, D. Gürlich, Strategies for cost efficient refurbishment and solar energy integration in European Case Study buildings, Energy Build. 102 (2015) 237–249, https://doi.org/10.1016/J.ENBUILD.2015.05.032.

[6] Q.W. Pan, Study on operation strategy of a silica gel-water adsorption chiller in solar cooling application, Sol. Energy 172 (2018) 24–31, https://doi.org/10.1016/J.SOLENER.2018.03.062.
[7] W. Chekirou, N. Boukheit, A. Karaali, Performance improvement of adsorption solar cooling system, Int. J. Hydrogen Energy 41 (2016) 7169–7174, https://doi.org/10.1016/J.IJHYDENE.2016.02.140.
[8] A. Mahesh, Solar collectors and adsorption materials aspects of cooling system, Renew. Sustain. Energy Rev. 73 (2017) 1300–1312, https://doi.org/10.1016/J.RSER.2017.01.144.
[9] Q.W. Pan, Z.Y. Xu, Solar-powered adsorption cooling systems, Adv. Sol. Heat Cool (2016) 299–328, https://doi.org/10.1016/B978-0-08-100301-5.00012-6.
[10] J. Asadi, P. Amani, M. Amani, A. Kasaeian, M. Bahiraei, Thermo-economic analysis and multi-objective optimization of absorption cooling system driven by various solar collectors, Energy Convers. Manag. 173 (2018) 715–727, https://doi.org/10.1016/J.ENCONMAN.2018.08.013.
[11] Z.Y. Xu, R.Z. Wang, Simulation of solar cooling system based on variable effect LiBr-water absorption chiller, Renew. Energy 113 (2017) 907–914, https://doi.org/10.1016/J.RENENE.2017.06.069.
[12] E. Bellos, C. Tzivanidis, Energetic and financial analysis of solar cooling systems with single effect absorption chiller in various climates, Appl. Therm. Eng. 126 (2017) 809–821, https://doi.org/10.1016/J.APPLTHERMALENG.2017.08.005.
[13] Z.Y. Xu, R.Z. Wang, Comparison of CPC driven solar absorption cooling systems with single, double and variable effect absorption chillers, Sol. Energy 158 (2017) 511–519, https://doi.org/10.1016/J.SOLENER.2017.10.014.
[14] D. Neyer, M. Ostheimer, N. Hauer, C. Halmdienst, W. Pink, Application of an adapted single-/half- effect NH3/H2O absorption chiller in tri-generation and solar cooling systems, Sol. Energy 173 (2018) 715–727, https://doi.org/10.1016/J.SOLENER.2018.08.010.
[15] T.S. Ge, R.Z. Wang, Z.Y. Xu, Q.W. Pan, S. Du, X.M. Chen, T. Ma, X.N. Wu, X.L. Sun, J.F. Chen, Solar heating and cooling: present and future development, Renew. Energy 126 (2018) 1126–1140, https://doi.org/10.1016/J.RENENE.2017.06.081.
[16] K. Bataineh, Y. Taamneh, Review and recent improvements of solar sorption cooling systems, Energy Build. 128 (2016) 22–37, https://doi.org/10.1016/J.ENBUILD.2016.06.075.
[17] U. Jakob, Solar cooling technologies, Renew. Heat Cool (2016) 119–136, https://doi.org/10.1016/B978-1-78242-213-6.00006-0.
[18] V. Brancato, A. Frazzica, Characterisation and comparative analysis of zeotype water adsorbents for heat transformation applications, Sol. Energy Mater. Sol. Cells 180 (2018) 91–102, https://doi.org/10.1016/J.SOLMAT.2018.02.035.
[19] V. Palomba, S. Vasta, G. Giacoppo, L. Calabrese, G. Gullì, D. La Rosa, A. Freni, Design of an innovative graphite exchanger for adsorption heat pumps and chillers, Energy Procedia (2015) 1030–1040, https://doi.org/10.1016/j.egypro.2015.12.112.
[20] A. Frazzica, V. Brancato, V. Palomba, S. Vasta, Sorption thermal energy storage, in: A. Frazzica, L.F. Cabeza (Eds.), Recent Adv. Mater. Syst. Therm. Energy Storage- an Introd. to Exp. Charact. Methods, Springer, 2019, pp. 33–54, https://doi.org/10.1007/978-3-319-96640-3_4.
[21] V. Palomba, B. Dawoud, A. Sapienza, S. Vasta, A. Frazzica, On the impact of different management strategies on the performance of a two-bed activated carbon/ethanol refrigerator: an experimental study, Energy Convers. Manag. 142 (2017), https://doi.org/10.1016/j.enconman.2017.03.055.
[22] A. Sapienza, V. Palomba, G. Gullì, A. Frazzica, S. Vasta, A new management strategy based on the reallocation of ads-/desorption times: experimental operation of a full-scale 3 beds adsorption chiller, Appl. Energy 205 (2017) 1081–1090, https://doi.org/10.1016/j.apenergy.2017.08.036.
[23] U. Bau, N. Baumgärtner, J. Seiler, F. Lanzerath, C. Kirches, A. Bardow, Optimal operation of adsorption chillers: first implementation and experimental evaluation of a nonlinear model-predictive-control strategy, Appl. Therm. Eng. (2018), https://doi.org/10.1016/J.APPLTHERMALENG.2018.07.078.
[24] A. Krajnc, J. Varlec, M. Mazaj, A. Ristić, N.Z. Logar, G. Mali, Superior performance of microporous aluminophosphate with LTA topology in solar-energy storage and heat reallocation, Adv. Energy Mater. 7 (2017) 1–8, https://doi.org/10.1002/aenm.201601815.
[25] A. Permyakova, S. Wang, E. Courbon, F. Nouar, N. Heymans, P. D'Ans, N. Barrier, P. Billemont, G. De Weireld, N. Steunou, M. Frère, C. Serre, Design of salt–metal organic framework composites for seasonal heat storage applications, J. Mater. Chem. A. 5 (2017) 12889–12898, https://doi.org/10.1039/C7TA03069J.
[26] F. Jeremias, A. Khutia, S.K. Henninger, C. Janiak, MIL-100(Al, Fe) as water adsorbents for heat transformation purposes—a promising application, J. Mater. Chem. 22 (2012) 10148–10151, https://doi.org/10.1039/C2JM15615F.
[27] A. Elsayed, E. Elsayed, R. AL-Dadah, S. Mahmoud, A. Elshaer, W. Kaialy, Thermal energy storage using metal–organic framework materials, Appl. Energy 186 (2017) 509–519, https://doi.org/10.1016/J.APENERGY.2016.03.113.
[28] A.D. Grekova, L.G. Gordeeva, Y.I. Aristov, Composite "LiCl/vermiculite" as advanced water sorbent for thermal energy storage, Appl. Therm. Eng. 124 (2017) 1401–1408, https://doi.org/10.1016/J.APPLTHERMALENG.2017.06.122.
[29] A.D. Grekova, L.G. Gordeeva, Z. Lu, R. Wang, Y.I. Aristov, Composite "LiCl/MWCNT" as advanced water sorbent for thermal energy storage: sorption dynamics, Sol. Energy Mater. Sol. Cells 176 (2018) 273–279, https://doi.org/10.1016/J.SOLMAT.2017.12.011.
[30] A. Grekova, L. Gordeeva, Y. Aristov, Composite sorbents "Li/Ca halogenides inside multi-wall carbon nano-tubes" for thermal energy storage, Sol. Energy Mater. Sol. Cells 155 (2016) 176–183, https://doi.org/10.1016/j.solmat.2016.06.006.
[31] D. Fröhlich, S.K. Henninger, C. Janiak, Multicycle water vapour stability of microporous breathing MOF aluminium isophthalate CAU-10-H, Dalton Trans. 43 (2014), https://doi.org/10.1039/c4dt02264e.
[32] E. Courbon, P. D'Ans, A. Permyakova, O. Skrylnyk, N. Steunou, M. Degrez, M. Frère, Further improvement of the synthesis of silica gel and CaCl2 composites: enhancement of energy storage density and stability over cycles for solar heat storage coupled with space heating applications, Sol. Energy 157 (2017) 532–541, https://doi.org/10.1016/J.SOLENER.2017.08.034.
[33] A. Fopah-Lele, C. Rohde, K. Neumann, T. Tietjen, T. Rönnebeck, K.E. N'Tsoukpoe, T. Osterland, O. Opel, W.K.L. Ruck, Lab-scale experiment of a closed thermochemical heat storage system including honeycomb heat exchanger, Energy 114 (2016) 225–238, https://doi.org/10.1016/J.ENERGY.2016.08.009.
[34] Á.G. Fernández, M. Fullana, L. Calabrese, E. Proverbio, L.F. Cabeza, Corrosion characterization in components for thermal energy storage applications, in: A. Frazzica, L.F. Cabeza (Eds.), Recent Adv. Mater. Syst. Therm. Energy Storage- an Introd. to Exp. Charact. Methods, Springer, 2019, pp. 139–169, https://doi.org/10.1007/978-3-319-96640-3_10.
[35] S. Longo, V. Palomba, M. Beccali, M. Cellura, S. Vasta, Energy balance and life cycle assessment of small size residential solar heating and cooling systems equipped with adsorption chillers, Sol. Energy 158 (2017) 543–558, https://doi.org/10.1016/j.solener.2017.10.009.
[36] B. Nienborg, A. Dalibard, L. Schnabel, U. Eicker, Approaches for the optimized control of solar thermally driven cooling systems, Appl. Energy 185 (2017) 732–744, https://doi.org/10.1016/J.APENERGY.2016.10.106.
[37] S. Vasta, V. Palomba, A. Frazzica, G. Di Bella, A. Freni, Techno-economic analysis of solar cooling systems for residential buildings in Italy, J. Sol. Energy Eng. Trans. ASME. 138 (2016), https://doi.org/10.1115/1.4032772.
[38] B. Delač, B. Pavković, K. Lenić, Design, monitoring and dynamic model development of a solar heating and cooling system, Appl. Therm. Eng. 142 (2018) 489–501, https://doi.org/10.1016/J.APPLTHERMALENG.2018.07.052.
[39] U. Eicker, D. Pietruschka, R. Pesch, Heat rejection and primary energy efficiency of solar driven absorption cooling systems´de l ' e´nergie primaire des Rejet de chaleur et efficacite ` mes de refroidissement a ` absorption faisant appel a syste´nergie solaire l ' e, Int. J. Refrig. 35 (2012) 729–738, https://doi.org/10.1016/j.ijrefrig.2012.01.012.
[40] M.H. Saidi, B. Sajadi, P. Sayyadi, Energy consumption criteria and labeling program of wet cooling towers in Iran, Energy Build. 43 (2011) 2712–2717, https://doi.org/10.1016/J.ENBUILD.2011.06.016.
[41] H.-M. Henning, J. Döll, Solar systems for heating and cooling of buildings, Energy Procedia 30 (2012) 633–653, https://doi.org/10.1016/j.egypro.2012.11.073.
[42] V. Palomba, S. Vasta, A. Freni, Q. Pan, R. Wang, X. Zhai, Increasing the share of renewables through adsorption solar cooling: a validated case study, Renew. Energy 110 (2017), https://doi.org/10.1016/j.renene.2016.12.016.
[43] A. Buonomano, F. Calise, A. Palombo, Solar heating and cooling systems by absorption and adsorption chillers driven by stationary and concentrating photovoltaic/thermal solar collectors: modelling and simulation, Renew. Sustain. Energy Rev. 82 (2018) 1874–1908, https://doi.org/10.1016/J.RSER.2017.10.059.
[44] E.G. Papoutsis, I.P. Koronaki, V.D. Papaefthimiou, Numerical simulation and parametric study of different types of solar cooling systems under Mediterranean climatic conditions, Energy Build. 138 (2017) 601–611, https://doi.org/10.1016/J.ENBUILD.2016.12.094.
[45] D. Neyer, M. Ostheimer, C. Dipasquale, R. Köll, Technical and economic assessment of solar heating and cooling – methodology and examples of IEA SHC Task 53, Sol. Energy 172 (2018) 90–101, https://doi.org/10.1016/J.SOLENER.2018.02.070.
[46] Pistache Tool, (n.d.).
[47] M. Imtiaz Hussain, C. Ménézo, J.-T. Kim, Advances in solar thermal harvesting technology based on surface solar absorption collectors: a review, Sol. Energy Mater. Sol. Cells 187 (2018) 123–139, https://doi.org/10.1016/J.SOLMAT.2018.07.027.
[48] K. Chopra, V.V. Tyagi, A.K. Pandey, A. Sari, Global advancement on experimental and thermal analysis of evacuated tube collector with and without heat pipe systems and possible applications, Appl. Energy 228 (2018) 351–389, https://doi.org/10.1016/J.APENERGY.2018.06.067.
[49] N.L. Batista, M.C. Rezende, E.C. Botelho, Effect of crystallinity on CF/PPS performance under weather exposure: moisture, salt fog and UV radiation, Polym. Degrad. Stabil. 153 (2018) 255–261, https://doi.org/10.1016/J.POLYMDEGRADSTAB.2018.03.008.
[50] AkoTec OEM Vario. https://akotec.eu/wp-content/uploads/18-01-Certificate-OEM-Vario-hp.pdf, 2016.
[51] J.A. Duffie, W.A. Beckman, Solar Engineering of Thermal Processes, Wiley, 2013.
[52] S. Vasta, V. Palomba, D. La Rosa, W. Mittelbach, Adsorption-compression cascade cycles: an experimental study, Energy Convers. Manag. 156 (2018) 365–375, https://doi.org/10.1016/j.enconman.2017.11.061.